

Position Matters: Sensor Placement for Sitting Posture Classification

Arpita Mallikarjuna Kappattanavar*, Harry Freitas da Cruz*, Bert Arnrich*, Erwin Böttinger*†

*Digital Health Center, Hasso Plattner Institute, University of Potsdam,
Prof.-Dr.-Helmert-Str. 2-3, 14482 Potsdam, Germany

†Hasso Plattner Institute for Digital Health at Mount Sinai

Icahn School of Medicine at Mount Sinai, New York, United States

Email: {Arpita.Kappattanavar|harry.freitasdacruz|bert.arnrich|erwin.boettinger}@hpi.de

Abstract—Prolonged sitting behavior and postures that cause strain on the spine and muscles have been reported to increase the probability of low back pain. To address this issue, many commercially available sensors already provide feedback about whether a person is ‘slouching’ or ‘not slouching’. However, they do not provide information on a person’s posture, which would give insights into the strain caused by a specific posture. Hence, in this pilot study, we attempt to find the optimum number of inertial measurement unit sensors required and the best locations to place them using six mock postures. Data is collected from these sensors and features are extracted. The number of features are reduced and the best features are selected using the Recursive Feature Elimination method with Cross-Validation. The reduced number of features is then trained and tested on Logistic Regression, Support Vector Machine and Hierarchical Model. Among the three models, the Support Vector Machine algorithm had the highest accuracy of 93.68%, obtained for the thoracic, hip and sacral region sensor combinations. While these findings will be validated in a larger study in an uncontrolled environment, this pilot study quantitatively highlights the importance of sensor placement in shaping discriminative performance in sitting posture classification tasks.

Index Terms—algorithm, classification, inertial measurement unit, location, recursive feature elimination, sitting posture

I. INTRODUCTION

Prolonged sitting behaviour and spine straining sitting postures have been reported to act as negative factors affecting health outcomes and which increases the probability of developing Low Back Pain (LBP) [1]–[5]. LBP is ranked as one of the top causes of sick leaves and an economic burden on health care system [6]. The proportion of people sitting for long hours during work and in their daily life has increased in recent years and around 75% of the employees in call centers, software companies and other industrial jobs spend on an average 90% of their workday sitting on a chair [1], [7], [8]. However, not all people spending 90% of their time sitting will develop chronic LBP. It is important to identify those particular postures or lifestyles which are associated with the chronification of LBP. Hence, to avoid it, maintaining a ‘good’ posture while sitting is essential [9].

Among other factors, treatment of low back pain requires an understanding of the mechanical factors potentially causing

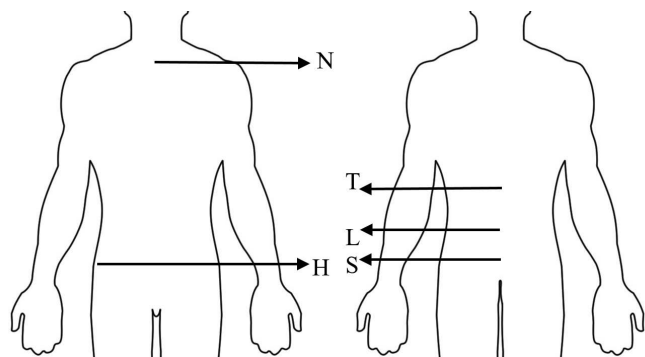


Fig. 1: Sensor locations on the human body in the Anterior View (AV) and Posterior View (PV). Abbreviations: T = 12th Thoracic vertebra, L = 3rd Lumbar vertebra, S= Between 1st and 2nd sacral vertebrae, H = Right hip, and N = Sternal angle.

the pain, such as spine movement [10], [11]. Hence, we concentrate on the movements performed by the spine as the person is sitting. There are different sitting postures considered to be optimal for a person based on the spinal curvature, intradiscal pressure, tissue stress and muscle activation [12], [13]. In order to identify the sitting postures leading to LBP, Inertial Measurement Unit (IMU) sensors are being used on the human body. Therefore, in this paper we present a pilot study to predict the optimum number and the best suited locations of IMU sensors to study both, the posture and the spine movement when a person is sitting. The aforementioned pilot study forms the basis for a larger study, which has been approved by the ethics commission of the University of Potsdam. It entails recording the sitting behaviors of subjects for 6-7 hours in his/her occupational settings, i.e., in an uncontrolled, real environment, enabling the results presented in this paper to be subsequently validated.

This work is organized as follows: In Section II, we present the related work, while in Section III we discuss our method. In Section IV, we present the results and discussion. Finally, in Section V we draw conclusions and provide an outlook on our future work.

II. RELATED WORK

IMU sensors have been placed on the upper and lower part of the back by Petropoulos et al. [14]. The angles extracted by each of the sensors were used to continuously monitor the sitting postures. Here, the authors have not mentioned the accuracy of the classification, and also the location of each sensor is randomly chosen in the upper and lower back. Sensor placement is an important step for the higher classification rate and lower hardware cost [15]. In order to understand the spine movement accurately, location of the sensor plays an important role as upper and lower lumbar spine regions demonstrate functional independence [16], [17]. The posture correcting devices commercially available, such as Upright Go [18] and Opter Pose [19] appear to be good posture correctors. However, both devices do not measure the movement of the spine, and only predict whether a person is ‘slouching’ or ‘not slouching’. Critically, little is known with respect to the correct location where to place these devices for enhanced accuracy.

III. METHODOLOGY

In the following section, we describe the tested locations for placement of the sensors, the pre-processing of the data and how the features were extracted and, the algorithms used for predicting different postures. The algorithms were programmed using the scikit-learn library [20].

A. Sensor Locations

We placed the Bonsai IMU sensors at five locations on the human body as shown in Figure 1. Three of the sensors were placed on the spine, at the 12th thoracic vertebra (T), 3rd lumbar vertebra (L), and between 1st and 2nd vertebrae of the sacral region (S) based on the previous literature [21]. The 4th sensor was placed at the right hip (H) and the fifth at the sternal angle (N) in order to check if it is convenient to place them in daily wearable. After positioning the sensors, the data was collected using the Logger app available on the iOS mobile application. The collected data were stored on the sensor module. The accelerometer and gyroscope data were retrieved from the sensor module.

Simultaneously, we placed two Kinect depth cameras as shown in Figure 2 to record the depth images of the upper and lower part of the body. These cameras were used as gold standards/labels for the classified data from the algorithms. Similar measurement setup is being used in the larger study to be carried out subsequently (already approved by ethics commission).

B. Study Protocol

Data collection was carried out on six subjects, five male and one female in the age group of 27-34 years, with weight and height in the range of 61-91 Kg and 169-180 cm respectively. All subjects signed the consent form to provide their data.

Initially, the sensors were placed on the subjects as shown in Figure 1. Then the subjects were made to sit for 3s to 5s. In order to help in the synchronisation of the data, the subjects

were made to stand up, jump and sit down straight. Thereafter, the subjects were instructed to sit in four different postures - forward, backward, lean right and lean left postures. Each instructed posture was repeated thrice with sitting-straight posture as the intermittent posture between the repetitions. Also, the sitting-straight posture was the intermittent posture during the transition from one posture to the other posture. The data was collected at a sampling frequency of 100 Hz for approximately six minutes for each subject.

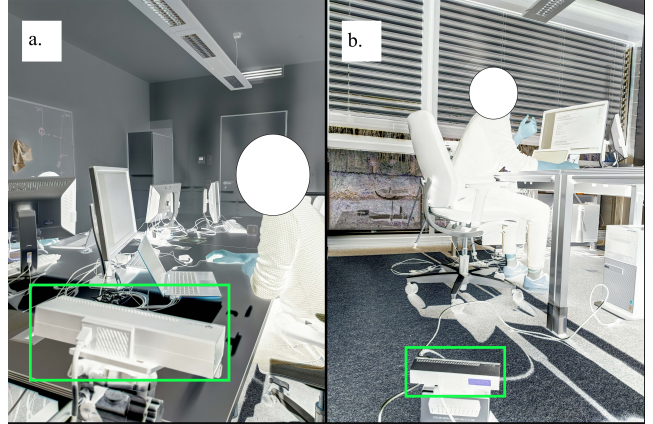


Fig. 2: The Kinect device set up for two cameras: a. records the upper body, while b. records the lower body.

C. Pre-processing

The synchronisation of the data from the five sensors was performed by aligning the peak data caused due to jumping. We labeled the data by watching the video. The labelling of transitions was challenging. However, we observed that the gyroscope data had peaks whenever there was transitions in the posture. Hence, the transitions were labelled using the magnitude of the g_x , g_y and g_z direction of the gyroscope data placed at the 12th thoracic region. The magnitude (M) was calculated using Equation 1 [22]:

$$M = \sqrt{g_x^2 + g_y^2 + g_z^2} \quad (1)$$

If $M > 0.7$, indicates transition and if $M < 0.7$, indicates no transition.

After the process of labelling, the raw data was first filtered using a nonlinear median filter. An odd window length of 151 was chosen for the median filter upon experimentation. The median filter reduced the spikes in the signal [23]. The filtered signal is windowed for 2s with 50% data overlap [24].

D. Feature Engineering

Based on the observation of the accelerometer data in the three axes (x, y, z), features were generated and extracted by finding the mean and standard deviation from each of the windows. We also performed correlations between the windows of two axes to extract features [24]. Correlation measures the similarity between two signals. Correlation between the same signal is called auto-correlation and between two different

signals it is called cross-correlation. Correlation is calculated using Equation 2 [25] :

$$R_{rr}[k] = \sum_{n=0}^N a_r[n]a_r[n - d] \quad (2)$$

where, a is the accelerometer signal, n is the index of the data sample, d is the displacement, $r = (p, q)$, p and q are the directions of the accelerometer (x, y, z), and the sensor locations (T, N, L, H, S) respectively. The maximum and minimum peak of the correlation were used as the features [25]. Similarly, pairwise correlation combinations of axes on different sensor combinations were performed using Equation 2, as these combinations improve recognition of activities involving movements of multiple body parts [16].

In the case of single sensors 18 features were extracted, in two sensor combinations 42 features, in three sensor combinations 66 features, in four sensors combinations 90 features and in five sensor combinations 113 features were extracted. As the number of sensors increased the features from the previous sensor combinations were also included in the increased sensor combinations. All the extracted features were normalized for their values to be between 0 and 1.

Algorithm 1: Recursive Feature Elimination Method

Result: Best rank features

Input: Training set X , Labels y ;

for each iteration **do**

Partition the training set and label into training data and test data via cross validation;

Train the model;

Predict the test data;

Calculate the feature ranking;

for Each subset of features F_i , $i = 1, \dots, f$ **do**

For ever iteration keep the F_i most important features;

Train the model using the F_i features;

Predict on the test data;

Recalculate the ranking of the features;

Calculate the accuracy over the F_i features using the test data samples;

Determine the appropriate number of features;

Estimate the final list of features for the final model;

Fit the model based on the best optimal number of features F_i using the original training set;

E. Feature Selection

According to the rule of thumb, the ratio of the number of training samples N to the number of features f , (N/f) must be at least ten [26]. The performance of a classification algorithm tends to critically depend on the dimension of the features considered in training the classifier. Hence, the number of extracted features had to be reduced for training the algorithm.

In order to reduce the number of features, the Recursive Feature Elimination (RFE) with Cross-Validation method with

multinomial Logistic Regression (LR) classifier and linear kernel Support Vector Machine (SVM) were used separately, to iteratively select the relevant features for the different sensor combinations. First, the subset of features from the training set were used for training the LR and SVM estimator. Then, the testing data were used for ranking the features. Weak features were eliminated at every step by fitting the model multiple times until all the features in the set were exhausted [27]. The best subset of features were selected based on the 6 fold cross-validation model score. The pseudocode for the RFE with cross-validation is presented in Algorithm 1 [28]. Table I presents the number of features extracted for each combinations.

F. Sensor Combinations and Algorithms

In order to minimize the number of sensors and find the best sensor locations to get good accuracy, different combinations of sensors were tested using the ‘combination without repetition formula’ and is presented in Equation 3 [29]:

$$C_{m,k} = \binom{m}{k} = \frac{m!}{k!(m-k)!} \quad (3)$$

where, m represents the total number of sensors and k the number of elements in a combination. Using Equation 3, 10 combinations were obtained for 2-set and 3-set sensors combinations each, 5 combinations for 1-set sensor combination, 5 combinations for 4-set sensor combination, and 1 combination for 5-set sensor. The reduced features using SVM model were used to train and test the LR, SVM and Hierarchical Model (HM) model.

1) *Multinomial Logistic Regression:* First, the basic Multinomial LR model was used for classification. The data was labeled into six classes $y \in \{1, 2, 3, 4, 5, 6\}$ where each of the class represents backward, forward, lean right, transition, lean left and sit straight postures respectively. The probability for each class was calculated using the `sklearn.linear_model.LogisticRegression` class from `scikit-learn` library [20].

2) *Support Vector Machine:* The classification in SVM is based on the optimal margins/boundaries created in the feature space [30]. These margins are created based on the support vectors. Since, this is a multi-class classification, ‘one-vs-rest’ approach is employed [31]. Hence six models were trained for six classes.

3) *Hierarchical Model:* It is a clustering algorithm in which nested clusters are formed [32]. The dendrogram tree was employed to identify the number of clusters or classes. In this study five, six, seven, eight, and nine clusters were identified for the different combinations. Since this study has six classes, six was applied as the number of clusters to the parameter in the class to cluster the training data. Then, for every test data the average euclidean distance was calculated with respect to each training data in a class. The test data is allocated to the class with which it has the minimum average distance.

The accuracy of these classifiers for different locations and their combinations were compared and is presented in Figure 3.

1 sensor combination	SVM Features	LR Features	4 sensors combination	SVM Features	LR Features
T	11	15	TNLH	19	76
N	7	18	TNLS	13	39
L	13	9	TNHS	12	44
H	10	14	TLHS	15	75
S	10	9	NLHS	72	87
2 sensors combination	SVM Features	LR Features	3 sensors combination	SVM Features	LR Features
TN	11	30	TNL	44	54
TL	37	38	TNH	31	15
TH	30	19	TNS	17	29
TS	27	17	TLH	21	23
NL	40	32	TLS	32	61
NH	11	17	THS	9	33
NS	11	35	NLH	59	53
LH	16	5	NLS	54	46
LS	41	31	NHS	30	40
HS	15	42	LHS	39	55

TABLE I: Number of features and their sensor combinations. Abbreviations: SVM = Support Vector Machine and LR = Logistic Regression. Note: The number of features varies with sensor location and its combinations

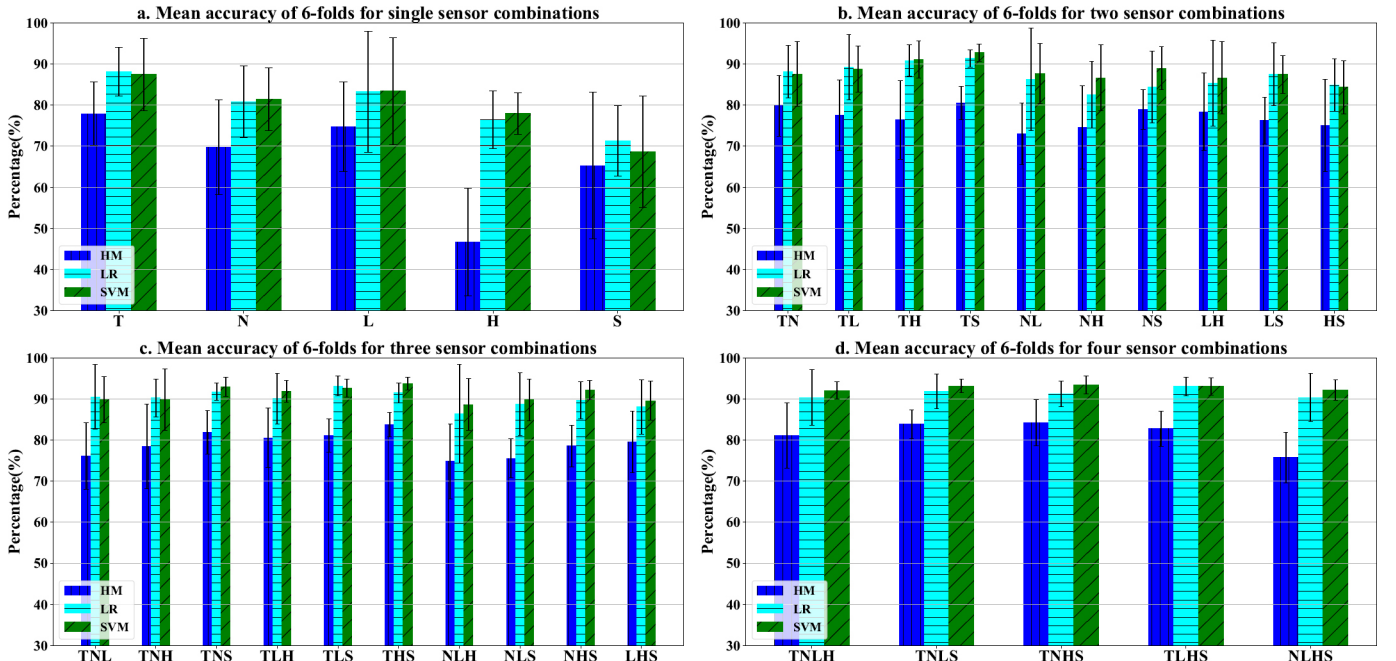


Fig. 3: Comparison of the mean and standard deviation of the classification accuracy of the 6-fold data for the one, two, three and four sensor combinations.

IV. RESULTS AND DISCUSSION

Table I shows the summary of the number of features after applying RFE for different combinations. Based on the observation of Table I, the reduced features obtained using SVM RFE were utilized for training and testing the other algorithms (SVM, LR, HM), as it had fewer features compared to LR RFE.

The mean and Standard Deviation (SD) of the classification accuracy of the 6-fold data obtained using reduced features for the three classification algorithms applied on one, two, three and four sensor combinations are presented in Figure 3. In the single sensor combinations presented in Figure 3.a, when the

sensor is at the T region of the spine, maximum accuracy of around 88% for LR and SVM, and 78% for HM was obtained. Yet, the SD for the LR was $\pm 5.919\%$ which was considerably less when compared to the other single sensor combinations displayed. However, there is a significant difference between the upper and lower back movements [16], [17]. As such, inputs from a single thoracic sensor can only be used to classify movements performed by the upper extremity of the back. Hence, in order to understand the spine movement there is a requirement of at least two sensors.

Figure 3.b presents 10 combinations of two sensors for the five locations. The maximum accuracy among the dif-

Feature Type	Region	Axis
Standard Deviation	Thoracic	x
		y
	Sacral	x
Maximum Peak Cross-correlation	Thoracic	x, y
		x, z
	Thoracic, Hip	y, x
Minimum Peak Cross-correlation	Thoracic	x, y
	Thoracic, Hip	y, x
Maximum Peak Auto-correlation	Thoracic	z

TABLE II: Nine most important features for the thoracic, hip and sacral region combination.

		Predicted					
		Backward	Forward	Sit right	Transition	Sit left	Sit straight
Actual	Backward	16	0	0	0	0	0
	Forward	0	16	0	0	0	0
	Sit right	0	0	17	1	0	0
	Transition	1	1	0	22	1	3
	Sit left	0	0	0	1	14	0
	Sit straight	0	0	0	2	0	71

Fig. 4: Confusion matrix for the thoracic, hip and sacral region combinations.

ferent combinations was obtained for those which included thoracic sensor. The maximum accuracy of 92.78%, 91.37% and 80.45% was obtained for SVM, LR and HM respectively at the thoracic, sacral region combinations. This accuracy obtained for SVM was almost 4% more than the single sensor combination. The SD obtained in this region was ± 2.12 , which is the lowest value of SD obtained for the 6-fold data for the 2 sensor combination. Accuracy increased when two sensors were used. However, the algorithm was trained using 27 features, which is more than double the number of features used in single sensor combination.

Three sensor combination is presented in Figure 3.c. The SVM and HM had its maximum accuracy of 93.68% and 83.76% respectively at the thoracic, hip and sacral region. The lowest SD of $\pm 1.54\%$ was obtained for SVM with only nine features presented in Table II, for differentiating the six postures as compared with the other two models for this combination. Table III and Figure 4 presents the discrimination metrics and confusion matrix respectively of the three sensor combination at the thoracic, hip and sacral region for the nine features. It can be observed from Table III that the total number of sitting straight is 73, which is more than the other 5 classes in this combination. This is due to the presence of many intermediate sittings between the postures. We can also observe that the recall, precision and F1 score was low during the transition. Therefore, in order to improve the performance of this model we need better features to identify transitions.

Posture	Recall	Precision	F1 Score	Total Data
Backward	0.94	1	0.97	16
Forward	0.94	1	0.97	16
Sit right	1	0.94	0.97	18
Transition	0.85	0.78	0.81	28
Sit left	0.93	0.93	0.93	15
Sit straight	0.96	0.97	0.96	73

TABLE III: Discrimination metrics for the thoracic, hip and sacral region combinations.

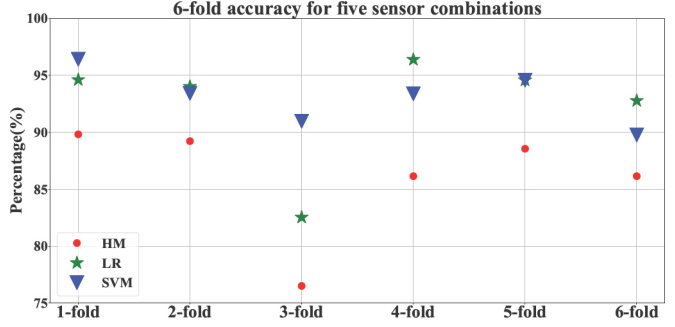


Fig. 5: Comparison of classification accuracy of the 6-folds for five sensor combination.

The 6-fold mean accuracy of the four sensor combinations is presented in Figure 3.d. Among the four sensor combinations, the combination of thoracic, neck, right hip and sacral region has given the maximum accuracy of 93.68% and 83.76% for SVM and HM respectively. Whereas for LR, the combination with thoracic, lumbar, right hip and sacral region has given the maximum accuracy of 93.08%. The accuracy of complete five sensor combination for the 6-folds is presented in Figure 5. It can be seen from the figure that the accuracy of the 5 sensors are consistent in SVM, LR and HM, with the exception of the 3rd fold. It can also be observed from Figure 5 that the results were more stable for SVM than the LR and HM, as the accuracy for SVM varied within 5% when compared to the other models which had approximately 10% variations at the 3rd fold. The average accuracy achieved for the 5 sensor combinations were 93.08%, 92.48% and 86.06% for SVM, LR and HM respectively. Thus, the accuracy, the SD and the number of features for the three sensor combinations at the thoracic, lumbar and sacral region for the SVM algorithm were better than all the other combinations and the other two models. It should also be noted that the number of features selected by the RFE method varies according to the placement of the sensors. For example SVM with three sensor combination ranged from 59 to 9 features. As such, we should further investigate what role under or overfitting might have played in the results. Such an analysis requires a larger cohort. Therefore, these findings will be validated in the larger study referred to previously.

V. CONCLUSION AND FUTURE WORK

This study suggests that the accuracy of sitting posture classification task also depends on the location and the optimal

number of IMU sensors, an aspect that has been insufficiently addressed in extant research. Moreover, the placement of a single sensor at the thoracic region seems to be a more favorable position when using only one sensor as compared with the other four locations in this study. However, the spine angles cannot be measured using a single sensor, since at least two are needed for this. Hence, the results indicate that the thoracic, hip and sacral region would be the ideal location for classifying the 6 mock postures. An increase in accuracy or a decrease in the SD or the number of features has not been observed for four and five sensor combinations. This points towards the fact that adding more sensors to the study may not help in improving the accuracy for the limited number of features. This generalization of the sensor location is limited, as this pilot study entails only six subjects participated in a controlled environment. Hence, these results are still subject to ulterior validation in the context of a fully fledged study, based on the classification of real life sitting postures in the occupational settings. Finally, we urge researchers in the field to conduct a careful evaluation to assess optimal sensor placement with respect to position and number, e.g., using the techniques described.

ACKNOWLEDGMENT

We would like to thank all the participants for contributing their data for this study, Juan Carlos Nino the medical doctor for the placement of the sensors at the right location, and Margaux Gatrio who helped us with data labeling. We would also like to thank Ariane Morassi Sasso for proofreading the paper.

REFERENCES

- [1] Carolin Bontrup et al. Low back pain and its relationship with sitting behaviour among sedentary office workers. *Appl. Ergon.*, 81:102894, nov 2019.
- [2] Karen H.E. Søndergaard, Christian G. Olesen, Eva K. Søndergaard, Mark de Zee, and Pascal Madeleine. The variability and complexity of sitting postural control are associated with discomfort. *J. Biomech.*, 43(10):1997–2001, jul 2010.
- [3] Nicolaas P. Pronk, Abigail S. Katz, Marcia Lowry, and Jane Rodmyre Payfer. Reducing Occupational Sitting Time and Improving Worker Health: The Take-a-Stand Project, 2011. *Prev. Chronic Dis.*, 9, oct 2012.
- [4] Angela Maria Lis, Katia M. Black, Hayley Korn, and Margareta Nordin. Association between sitting and occupational LBP. *Eur. Spine J.*, 16(2):283–298, feb 2007.
- [5] Chiung Yu Cho, Yea Shwu Hwang, and Rong Ju Cherng. Musculoskeletal symptoms and associated risk factors among office workers with high workload computer use. *J. Manipulative Physiol. Ther.*, 35(7):534–540, sep 2012.
- [6] Christina M. Wenig, Carsten O. Schmidt, Thomas Kohlmann, and Bernd Schweißert. Costs of back pain in Germany. *Eur. J. Pain*, 13(3):280–286, mar 2009.
- [7] Leon Straker and Svend Erik Mathiassen. Increased physical work loads in modern work - A necessity for better health and performance? *Ergonomics*, 52(10):1215–1225, 2009.
- [8] "Standing or walking versus sitting on the job in 2016 : The Economics Daily: U.S. Bureau of Labor Statistics," 01-Mar-2017. [Online]. Available: <https://www.bls.gov/opub/ted/2017/standing-or-walking-versus-sitting-on-the-job-in-2016.htm>. [Accessed: 03-Oct-2019].
- [9] CC Lim, SN Basah, MA Ali, and CY Fook. Wearable posture identification system for good sitting position. *Journal of Telecommunication, Electronic and Computer Engineering (JTEC)*, 10:135–140, 2018.
- [10] Stuart M McGill. Low back exercises: evidence for improving exercise regimens. *Physical therapy*, 78(7):754–765, 1998.
- [11] Enrica Papi, Woon Senn Koh, and Alison H. McGregor. Wearable technology for spine movement assessment: A systematic review. *J. Biomech.*, 64:186–197, nov 2017.
- [12] Arnold Y. L. Wong et al. Do different sitting postures affect spinal biomechanics of asymptomatic individuals? *Gait Posture*, 67:230–235, jan 2019.
- [13] Raquel Castanharo, Marcos Duarte, and Stuart McGill. Corrective sitting strategies: An examination of muscle activity and spine loading. *J. Electromyogr. Kinesiol.*, 24(1):114–119, feb 2014.
- [14] Anastasios Petropoulos, Dimitrios Sikeridis, and Theodore Antonakopoulos. SPOMo: IMU-based real-Time sitting posture monitoring. *IEEE Int. Conf. Consum. Electron. - Berlin, ICCE-Berlin*, 2017-Septe:5–9, 2017.
- [15] Bilge Mutlu, Andreas Krause, Jodi Forlizzi, Carlos Guestrin, and Jessica Hodgins. Robust, low-cost, non-intrusive sensing and recognition of seated postures. In *UIST Proc. Annu. ACM Symp. User Interface Software Technol.*, pages 149–158, 2007.
- [16] Ling Bao and Stephen S. Intille. Activity recognition from user-annotated acceleration data. *Lect. Notes Comput. Sci. (including Subser. Lect. Notes Artif. Intell. Lect. Notes Bioinformatics)*, 3001:1–17, 2004.
- [17] Kieran O'Sullivan, Raymond McCarthy, Alison White, Leonard O'Sullivan, and Wim Dankaerts. Lumbar posture and trunk muscle activation during a typing task when sitting on a novel dynamic ergonomic chair. *Ergonomics*, 55(12):1586–1595, dec 2012.
- [18] "How To Improve Posture With Upright - Fix Bad Posture Fast!," UP-RIGHT, 2020. [Online]. Available: <https://www.uprightpose.com/how-it-works/>. [Accessed: 21- Jan- 2020].
- [19] "Opter Pose – Your Connected Wearable for Posture Correction and More," Opterlife.com, 2020. [Online]. Available: <https://opterlife.com/>. [Accessed: 21- Jan- 2020].
- [20] Fabian Pedregosa, Vincent Michel, and Olivier Grisel et al. Scikit-learn: Machine Learning in Python. Technical report, 2011.
- [21] Kieran O'Sullivan, Peter O'Sullivan, Leonard O'Sullivan, and Wim Dankaerts. What do physiotherapists consider to be the best sitting spinal posture? *Man. Ther.*, 17(5):432–437, oct 2012.
- [22] A R Jiménez, F Seco, J C Prieto, and J Guevara. Indoor Pedestrian Navigation using an INS/EKF framework for Yaw Drift Reduction and a Foot-mounted IMU. Technical report, 2010.
- [23] Élcio Jerônimo de Oliveira, Elio Koiti Kuga, and Ijar Milagre da Fonseca. IMU Fault Detection Based on χ^2 -CUSUM. *Math. Probl. Eng.*, 2012:15.
- [24] Sara Saeedi and Naser El-Sheimy. Activity recognition using fusion of low-cost sensors on a smartphone for mobile navigation application. *Micromachines*, 6(8):1100–1134, 2015.
- [25] Suryannarayana Chandaka, Amitava Chatterjee, and Sugata Munshi. Support vector machines employing cross-correlation for emotional speech recognition. *Meas. J. Int. Meas. Confed.*, 42(4):611–618, may 2009.
- [26] Andrea Mannini and Angelo Maria Sabatini. Machine learning methods for classifying human physical activity from on-body accelerometers. *Sensors*, 10(2):1154–1175, feb 2010.
- [27] Hosik Choi, Donghwa Yeo, Sunghoon Kwon, and Yongdai Kim. Gene selection and prediction for cancer classification using support vector machines with a reject option. *Comput. Stat. Data Anal.*, 55(5):1897–1908, may 2011.
- [28] Max Kuhn et al. Building predictive models in r using the caret package. *Journal of statistical software*, 28(5):1–26, 2008.
- [29] David R. Mazur. *Combinatorics: a guided tour*, volume 47. American Library Association, june 2010.
- [30] Vladimir Naumovich. *Statistical learning theory*. Wiley, 1998.
- [31] Jiayu Chen, Jun Qiu, and Changbum Ahn. Construction worker's awkward posture recognition through supervised motion tensor decomposition. *Autom. Constr.*, 77:67–81, may 2017.
- [32] Laura Igual and Santi Seguí. Introduction to Data Science. pages 1–4, 2017.